International Journal of Bifurcation and Chaos, Vol. 24, No. 8 (2014) 1440013 (9 pages)
© World Scientific Publishing Company
DOI: 10.1142/S0218127414400136

When Transitions Between Bursting Modes Induce Neural Synchrony

Reimbay Reimbayev and Igor Belykh*
Department of Mathematics and Statistics, and Neuroscience Institute, Georgia State University, 30 Pryor Street, Atlanta, GA 30303, USA
**ibelykh@gsu.edu*

Received February 2, 2014

We study the synchronization of bursting cells that are coupled through both excitatory and inhibitory connections. We extend our recent results on networks of Hindmarsh–Rose bursting neurons [Belykh *et al.*, 2014] to coupled Sherman β-cell models and show that the addition of repulsive inhibition to an excitatory network can induce synchronization. We discuss the mechanism of this purely synergenic phenomenon and demonstrate that the inhibition leads to the disappearance of a homoclinic bifurcation that governs the type of synchronized bursting. As a result, the inhibition causes the transition from square-wave to easier-to-synchronize plateau bursting, so that weaker excitation is sufficient to induce bursting synchrony. We dedicate this paper to the memory of Leonid P. Shilnikov, the pioneer of homoclinic bifurcation theory, and emphasize the importance of homoclinic bifurcations for understanding the emergence of synchronized rhythms in bursting networks.

Keywords: Bursting; synchronization; inhibition; excitation; neural networks.

1. Introduction

Neurons can generate complex patterns of bursting activity. Over the last thirty years, much work has been dedicated to the classification of bursting rhythms [Rinzel, 1987; Rinzel & Ermentrout, 1989; Bertram *et al.*, 1995; Izhikevich, 2000; Golubitsky *et al.*, 2001] and the bifurcation transitions between them (see [Terman, 1991, 1992; Wang, 1993; Belykh *et al.*, 2000; Shilnikov *et al.*, 2005; Frohlich & Bazhenov, 2006] and references therein). This includes chaotic bursting [Guckenheimer & Oliva, 2002] and transitions between tonic spiking and bursting, caused by homoclinic bifurcations of a saddle-node periodic orbit and the blue sky catastrophe [Turaev & Shilnikov, 1995; Shilnikov & Cymbaluyk, 2005].

When coupled in a network, bursting neurons can attain different forms of synchrony: burst synchronization when only the envelopes of the spikes synchronize, complete synchrony, anti-phase bursting, and other forms of phase-locking. The emergence of a specific cooperative rhythm depends on the intrinsic properties of the coupled neurons, a type and strength of synaptic coupling, and network circuitry [Wang & Rinzel, 1992; van Vreeswijk *et al.*, 1994; Kopell & Ermentrout, 2002; Elson *et al.*, 2002; Somers & Kopell, 1993; Sherman, 1994; Canavier *et al.*, 1999; Rubin & Terman, 2002; Kopell & Ermentrout, 2004; Belykh *et al.*, 2005; Izhikevich, 2001; Belykh & Shilnikov, 2008; Shilnikov *et al.*, 2008; Wojcik *et al.*, 2011; Wojcik *et al.*, 2014]. Fast excitatory synapses are known to

*Author for correspondence

facilitate bursting synchrony (see [Kopell & Ermentrout, 2004; Izhikevich, 2001; Belykh *et al.*, 2005]). However, fast inhibition typically leads to anti-phase or asynchronous bursting [Wang & Rinzel, 1992; Rubin & Terman, 2002; Belykh & Shilnikov, 2008], unless the inhibitory connections are weak and the initial conditions are chosen close enough together within the spiking phase of bursting [Jalil *et al.*, 2012]. Making excitatory and inhibitory synapses slower reverses their roles such that inhibition, not excitation leads to bursting synchrony [van Vreeswijk *et al.*, 1994; Elson *et al.*, 2002].

In a recent paper [Belykh *et al.*, 2014], we studied networks of phenomenological Hindmarsh–Rose neuron models [Hindmarsh & Rose, 1984] and discovered a counterintuitive effect that fast, desynchronizing inhibition can induce synchronized bursting when added to an excitatory network of square-wave bursters. This nontrivial phenomenon appears as a result of a synergetic interaction between synchronizing excitation and desynchronizing inhibition. Its key component is the ability of inhibition to effectively change the type of bursting in the network, switching from square-wave to plateau-type bursting. Consequently, significantly less excitation is necessary to trigger network synchronization. In this paper, we demonstrate that a similar effect is observed in a network of physiologically-based Hodgkin–Huxley-type models such as the pancreatic β-cell Sherman model [Sherman, 1994], exhibiting square-wave and plateau-type bursting. Square-wave bursting [Rinzel, 1987] was named after the shape of the voltage trace during a burst; it resembles a square wave due to fast transitions between the quiescent state and fast repetitive spiking (see Fig. 1). Square-wave bursters are notorious for their resistance to synchronization and require strong excitatory coupling to synchronize them. In the Izhikevich classification [Izhikevich, 2000], square-wave bursters, observed in the Sherman model, correspond to an Andronov–Hopf/homoclinic burster. Its main signature is the presence of a homoclinic bifurcation of a saddle in the 2-D fast subsystem. In the following, we will show that the addition of inhibition induces synchrony by making this homoclinic bifurcation disappear and generating plateau-type bursting (Andronov–Hopf/Andronov–Hopf bursting, according to the Izhikevich classification).

Homoclinic bifurcation theory was primarily developed by Leonid Pavlovich Shilnikov. By this

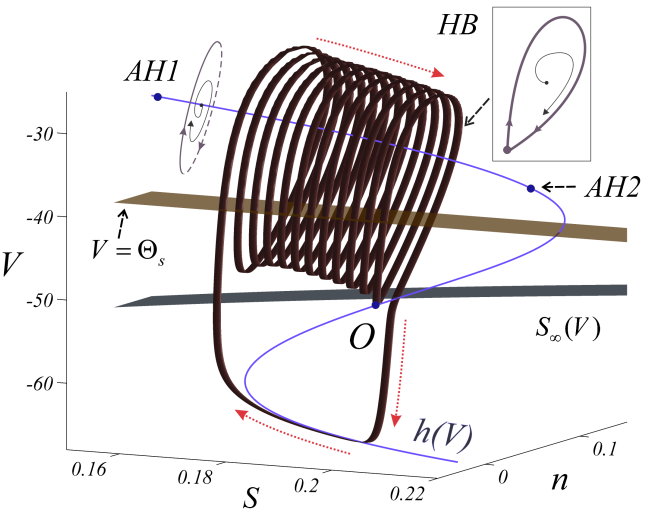

Fig. 1. Square-wave burster of the uncoupled Sherman models (1). The fast system displays a supercritical Andronov–Hopf bifurcation at $S = S_{\rm AH1}$ and a homoclinic bifurcation (loop) at $S = S_{\rm HB}$. The spiking manifold is composed of limit cycles in the fast system and terminates at the homoclinic bifurcation HB. The intersection of the fast ($h(V)$) and slow ($S_\infty(V)$) nullclines indicates a unique saddle point O of the full system. The red dotted curve shows the route for bursting in the full system. The plane $V = \Theta_s$ displays the synaptic threshold above which the presynaptic cell can influence the postsynaptic one.

paper, we pay tribute to his pioneering contributions [Shilnikov *et al.*, 1998; Shilnikov *et al.*, 2001] and argue that homoclinic bifurcations continue to be a source of unexpected phenomena in both single and coupled bursting cell models.

The layout of this paper is as follows. First, in Sec. 2, we introduce the network model and the Sherman cell model as its individual unit. We show that the uncoupled cell model exhibits square-wave bursting and discuss the generation mechanism. Then, in Sec. 3, we introduce the self-coupled system that governs the type of synchronous bursting. We show that the self-coupled system switches from square-wave to plateau bursting with an increase in the excitatory and/or inhibitory couplings. This property is then used in Sec. 4 to analyze the variational equations for the transverse stability of the synchronous bursting solution, defined through the self-coupled system. Several stability arguments are given to explain the synergetic, synchronizing effect of combined excitation and inhibition. In Sec. 5, similar transitions to synchronized plateau-bursting are shown in a network with a varying reversal potential. Finally, in Sec. 6, a brief discussion of the obtained results is given.

2. The Network Model

We consider the simplest network of two coupled Sherman models with both excitatory and inhibitory connections:

$$\begin{aligned}
\tau\frac{dV_i}{dt} &= F(V_i, n_i, S_i) + g_{\text{exc}}(E_{\text{exc}} - V_i)\Gamma(V_j) \\
&\quad + g_{\text{inh}}(E_{\text{inh}} - V_i)\Gamma(V_j), \\
\tau\frac{dn_i}{dt} &= G(V_i, n_i) \equiv n_\infty(V_i) - n_i, \\
\tau_s\frac{dS_i}{dt} &= H(V_i, S_i) \equiv S_\infty(V_i) - S_i, \quad i, j = 1, 2.
\end{aligned} \tag{1}$$

Here, V_i represents the membrane potential of the ith cell. Function $F(V_i, n_i, S_i) = -[I_{\text{Ca}}(V_i) + I_{\text{K}}(V_i, n_i) + I_{\text{S}}(V_i, S_i)]$ defines three intrinsic currents: fast calcium, I_{Ca}, potassium, I_{K}, and slow potassium, I_{S}, currents:

$$\begin{aligned}
I_{\text{Ca}} &= \bar{g}_{\text{Ca}} m_\infty(V_i)(V_i - E_{\text{Ca}}), \\
I_{\text{K}} &= \bar{g}_{\text{K}} n_i (V_i - E_{\text{K}}), \\
I_{\text{S}} &= \bar{g}_{\text{S}} S_1 (V_i - E_{\text{K}}).
\end{aligned}$$

The gating variables for n_i and S_i are the opening probabilities of the fast and slow potassium currents, respectively, and

$$\begin{aligned}
m_\infty(V_i) &= \left[1 + \exp\left(\frac{-20 - V_i}{12}\right)\right]^{-1} \\
n_\infty(V_i) &= \left[1 + \exp\left(\frac{-16 - V_i}{5.6}\right)\right]^{-1} \\
S_\infty(V_i) &= \left[1 + \exp\left(\frac{-35.245 - V_i}{10}\right)\right]^{-1}.
\end{aligned}$$

Other intrinsic parameters are $\tau = 20$, $\tau_{\text{S}} = 10\,000$, $\bar{g}_{\text{Ca}} = 3.6$, $E_{\text{Ca}} = 25\,\text{mV}$, $\bar{g}_{\text{K}} = 10$, $E_{\text{K}} = -75\,\text{mV}$, $\bar{g}_{\text{S}} = 4$.

The cells are identical and the symmetrical synaptic connections are fast and instantaneous. The parameters g_{exc} and g_{inh} are the excitatory and inhibitory coupling strengths. The reversal potentials $E_{\text{exc}} = 10\,\text{mV}$ and $E_{\text{inh}} = -75\,\text{mV}$ make the synapses excitatory and inhibitory, respectively as $E_{\text{exc}} > V_i$ ($E_{\text{inh}} < V_i$) for all values of $V_i(t)$. The synaptic coupling function is modeled by the sigmoidal function $\Gamma(V_j) = 1/[1+\exp\{-10(V_j - \Theta_s)\}]$. The synaptic threshold $\Theta_{\text{syn}} = -40\,\text{mV}$ is set to ensure that every spike in the single cell burst can reach the threshold (see Fig. 1). As a result, a spike arriving from a presynaptic cell j activates the synapse current (through $\Gamma(V_j)$ switching from 0 to 1) entering the postsynaptic cell i. Unless noticed otherwise, we will keep the above parameters fixed and only vary the synaptic strengths g_{exc} and g_{inh}.

The presence of the large parameter $\tau_S = 10\,000$ on the left-hand side of the S-equation makes the system (1) slow–fast such that the (V_i, n_i)-equations represent the 2-D fast "spiking" subsystem for the ith cell; the S_i-equation corresponds to the slow 1-D "bursting" system. Therefore, we use the standard decomposition into fast and slow subsystems; the types of bursting that can exist in the uncoupled cell systems (1) with $g_{\text{exc}} = 0$ and $g_{\text{inh}} = 0$ are defined by the S-parameter sequences of phase portraits of the 2-D fast system. This analysis has been performed for a similar pancreatic cell [Tsaneva-Atanasova *et al.*, 2010] and revealed different types of bursting such as square-wave, plateau and pseudo-plateau bursting [Stern *et al.*, 2008]. Figure 1 illustrates the standard sequence of phase portraits in the uncoupled systems (1) with $g_{\text{exc}} = 0$ and $g_{\text{inh}} = 0$, giving rise to square-wave bursting.

The equilibrium point on the upper branch of the nullcline $h(V)$ in the 2-D fast subsystem undergoes a supercritical Andronov–Hopf bifurcation for $S = S_{\text{AH1}}$, softly giving rise to a stable limit cycle that encircles the unstable point and forms the spiking manifold for $S_{\text{AH1}} < S < S_{\text{HB}}$. Its upper edge is defined by a homoclinic bifurcation at $S = S_{\text{HB}}$. Here, the stable limit merges into a stable homoclinic loop and disappears. For the given location of the slow nullcline $S_\infty(V)$, the trajectories jump down to the lower branch of the fast nullcline, creating square-wave (fold/homoclinic) bursting. A more detailed analysis of the phase portraits' sequences and bifurcations leading to square-wave bursting in other cell models such as the Hindmarsh–Rose model can be found in [Shilnikov & Kolomiets, 2008; Belykh & Hasler, 2011].

3. Self-Coupled System and Its Burster

Each cell in the network (1) receives one inhibitory and one exciatory input from the other cell, therefore the network system (1) has an invariant manifold $D = \{V_1 = V_2 = V(t), n_1 = n_2 = n(t),$

$S_1 = S_2 = S(t)\}$, that defines complete synchronization between the cells.

Synchronous dynamics on the manifold D is defined by the self-coupled system:

$$\begin{aligned}\tau\frac{dV}{dt} &= F(V,n,S) + g_{\rm exc}(E_{\rm exc}-V)\Gamma(V)\\ &\quad + g_{\rm inh}(E_{\rm inh}-V)\Gamma(V),\\ \tau\frac{dn}{dt} &= G(V,n)\\ \tau_s\frac{dS}{dt} &= H(V,S).\end{aligned} \tag{2}$$

Note that the synchronous dynamics differs from that of the uncoupled cell as the former is governed by a system with extra coupling terms. Moreover, the synchronous dynamics and the type of bursting depend on the coupling strengths $g_{\rm exc}$ and $g_{\rm inh}$. There are critical coupling strengths $g_{\rm exc}$ and $g_{\rm inh}$ at which square-wave bursting in the self-coupled system (2) turns into plateau-type bursting, depicted in Fig. 2. This happens through the disappearance of the homoclinic bifurcation in the self-coupled system (2) due to increased coupling strengths.

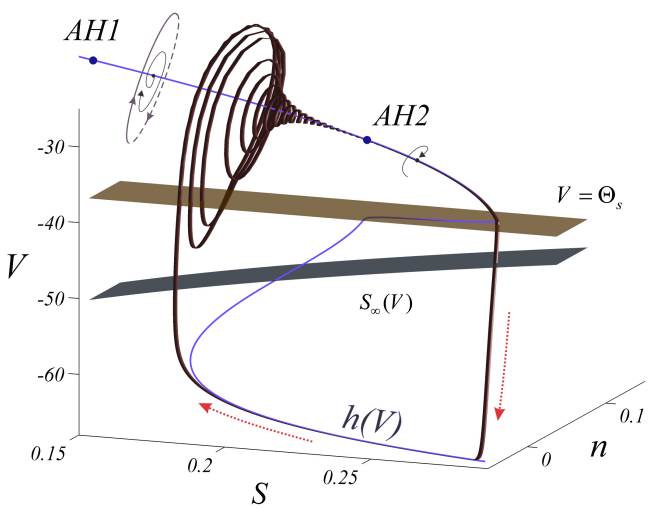

Fig. 2. Plateau-type burster of the self-coupled model (2), governing the synchronous network dynamics. Note the disappearance of a homoclinic bifurcation in the fast system due to the synaptic coupling. The stable limit cycle of the fast system disappears through a reverse Andronov–Hopf bifurcation at $S = S_{\rm AH2}$, ending the spiking manifold. The red dotted curve shows the route for plateau-type bursting. The nonsmooth part of the fast nullcline at $V = \Theta_s$ is due to the synaptic coupling, turning on when the trajectory jumps up to the spiking manifold and crosses the threshold Θ_s. The coupling strengths $g_{\rm exc} = 0.14$ and $g_{\rm inh} = 0.06$ correspond to the point b in the 2-D diagram of Fig. 3.

In the following, we will show that the disappearance of the homoclinic bifurcation (HBD) practically coincides with the onset of stable synchrony in the system (1). While excitation alone is able to transform square-wave into plateau-type bursting at some high values of $g_{\rm exc}$, inhibition does so more effectively and its addition lowers the combined coupling strength $g_{\rm exc} + g_{\rm inh}$.

4. Stability of Synchronization: A Synergetic Effect of Inhibition and Excitation

The stability of synchronization in the network (1) is equivalent to the stability of the invariant manifold D. The variational equations for its infinitesimal transverse perturbations $\Delta V = V_1 - V_2$, $\Delta n = n_1 - n_2$, and $\Delta S = S_1 - S_2$ read [Belykh *et al.*, 2005; Belykh *et al.*, 2014]:

$$\begin{aligned}\tau\frac{d}{dt}\Delta V &= F_V(V,n,S)\Delta V + F_n(V,n,S)\Delta n\\ &\quad + F_S(V,n,S)\Delta S - \Omega(V)\Delta V\\ \tau\frac{d}{dt}\Delta n &= G_V(V,n)\Delta V + G_n(V,n)\Delta n\\ \tau\frac{d}{dt}\Delta S &= H_V(V,S)\Delta V + H_S(V,S)\Delta S,\end{aligned} \tag{3}$$

where

$$\begin{aligned}\Omega(V) &= (g_{\rm exc}+g_{\rm inh})\Gamma(V) + (g_{\rm exc}(E_{\rm exc}-V)\\ &\quad + g_{\rm inh}(E_{\rm inh}-V))\Gamma_V(V).\end{aligned} \tag{4}$$

Here, the partial derivatives are calculated at the point $\{\Delta V = 0, \Delta n = 0, \Delta S = 0\}$; and $\{V(t), n(t), S(t)\}$ is the synchronous bursting solution defined through the system (2). Note that the synaptic coupling function $\Gamma(V)$ along with its derivative $\Gamma_V(V) = \frac{\lambda\exp\{-\lambda(V-\Theta_s)\}}{(1+\exp\{-\lambda(V-\Theta_s)\})^2}$ is non-negative. Hence, the contribution of the first term in (4), $-(g_{\rm exc} + g_{\rm inh})\Gamma(V)\Delta V$ is stabilizing for the zero fixed point of the variational system (3), corresponding to synchronous bursting. On the other hand, the contribution of the second coupling term in (4) can be destabilizing when $g_{\rm inh}(E_{\rm inh} - V)$ exceeds $g_{\rm exc}(E_{\rm inh} - V)$, making the second term overall negative. Note that increasing the inhibitory coupling $g_{\rm inh}$ makes this term more negative and, therefore, promoting desynchronization as one would expect. However, Fig. 3(a) indicates that the addition of inhibition to an excitatory network

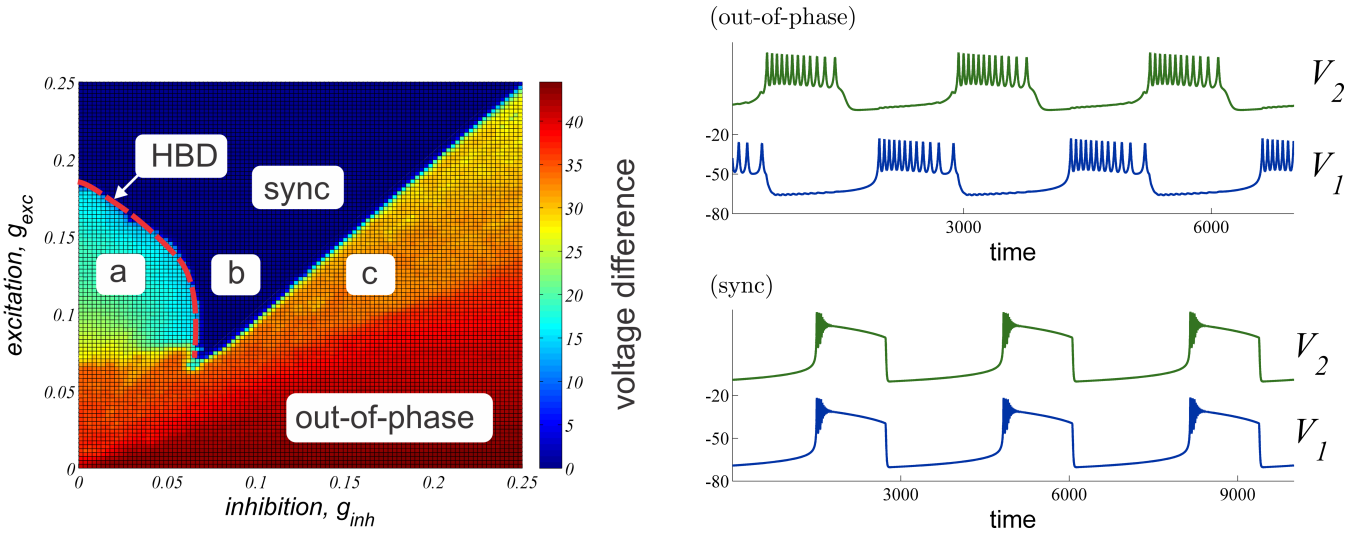

(a) (b)

Fig. 3. (a) The stability diagram for synchronization in the two-cell network (1). The color bar indicates the maximum voltage difference $V_1 - V_2$, calculated over the last two bursts in the established rhythm. Blue (dark) zone corresponds to the zero voltage difference and shows the synchronization region. Note the unexpected effect when an increase of the inhibitory coupling from 0 to 0.07 significantly lowers the synchronization threshold from about 0.18 to 0.07. Notice that the inhibition desynchronizes the cells in the absence of excitation ($g_{\rm exc} = 0$). The red dashed curve indicates the disappearance of the homoclinic bifurcation (HBD) in the 2-D fast subsystem; it corresponds to the transition from square-wave to plateau bursting and practically coincides with the stability boundary between asynchronized and synchronized bursting. (b) (Top) Typical out-of-phase voltage traces, corresponding to the red ("out-of-phase") zone. (Bottom) Synchronization of plateau bursting in the blue ("sync") parameter region.

induces synchronization in a fairly wide range of the inhibitory strength $g_{\rm inh}$. Note that increasing $g_{\rm inh}$ first lowers the synchronization threshold and weaker excitation synchronizes the cells (e.g. from $g_{\rm exc} = 0.18$ in the absence of inhibition to $g_{\rm exc} = 0.07$ for $g_{\rm inh} = 0.07$). At the same time, the inhibition cannot induce robust synchronization by itself (see the x-axis in Fig. 3(a), which corresponds to the desynchronizing role of inhibition in the absence of excitation).

What is the cause of this highly unexpected phenomenon? It is worth noticing that when complete (spike) synchronization occurs in the purely excitatory network (1) with $g_{\rm inh} = 0$, square-wave bursting, observed in the unsynchronized network (1) at lower values of $g_{\rm exc}$, turns into plateau bursting [see Fig. 3(b)]. This happens when the excitatory coupling is strong enough to change the type of bursting via the disappearance of the homoclinic bifurcation in the fast subsystem of (2). The important ingredient of the inhibition-induced synchronization in the network is that the inhibition changes the type of bursting much more effectively than the excitation [see Fig. 3(a)]. Consequently, a much smaller amount of the combined force ($g_{\rm exc} + g_{\rm inh}$) is necessary for synchronization.

Why is plateau bursting easier to synchronize? Why does inhibition not desynchronize plateau oscillations as it seems to have an apparent destabilizing effect due to the second term in (4)?

These questions have been answered for networks of Hindmarsh–Rose models in our recent paper [Belykh *et al.*, 2014]; here, we give additional details and adapt the main arguments to the network of Sherman models (1), representing realistic Hodgkin–Huxley-type cell models. Figure 4 answers these questions by revealing the dynamics and stability of synchronous bursting via the variational system (3) and self-coupled system (2), describing the synchronous solution $V(t)$, whether stable or unstable. Figure 4(a)(top) shows the synchronous solution of the self-coupled system (2), which is unstable as the coupling is not sufficiently strong [see the corresponding point a in Fig. 3(a)]. The contribution of the coupling term $\Omega(V)$ to the stabilization of the synchronous solution is depicted in Fig. 4(a)(bottom). When the voltage is above the synaptic threshold $\Theta_{\rm s}$, only the first (stabilizing)

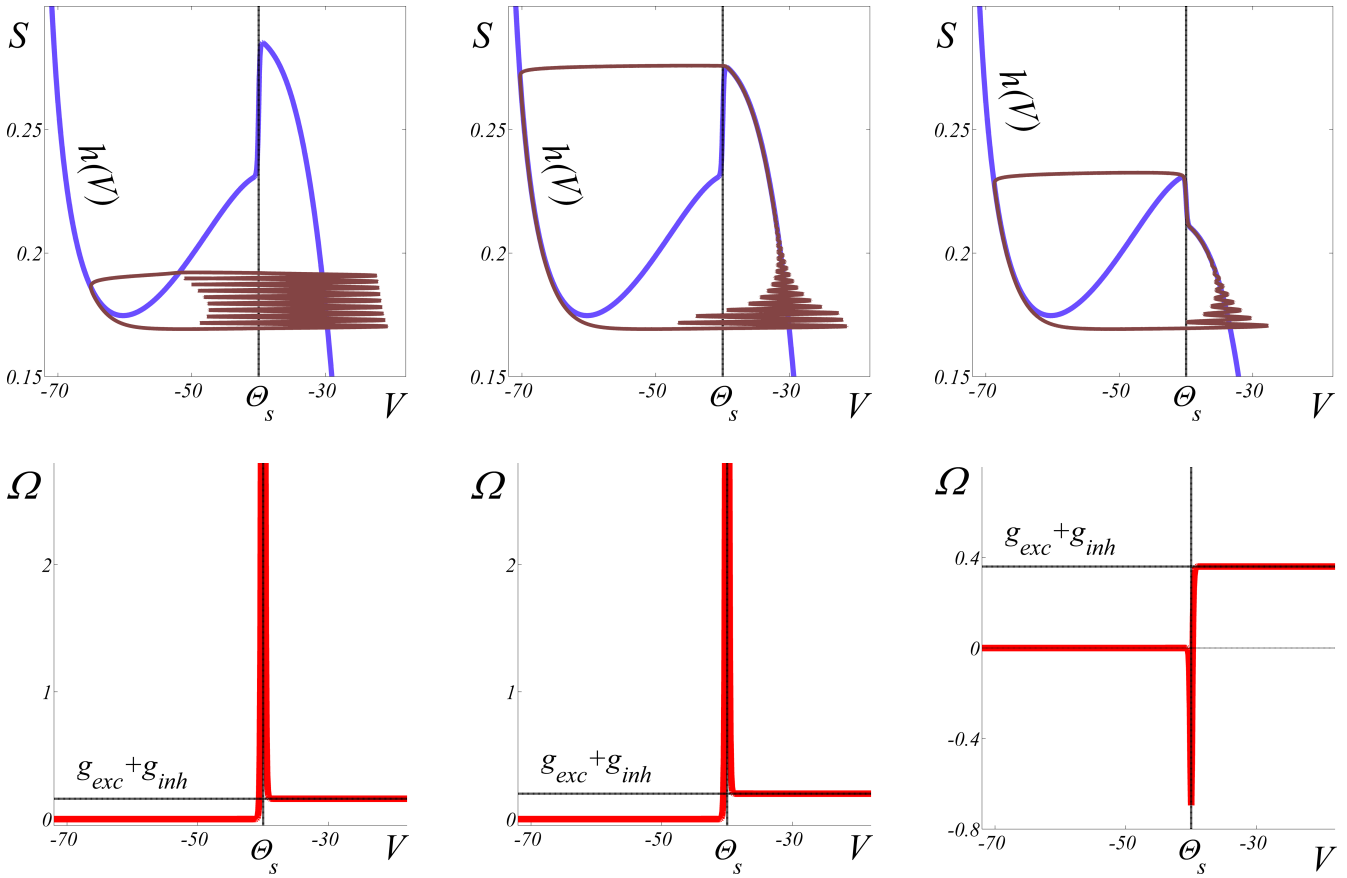

Fig. 4. The role of inhibition in the stability and type of synchronous bursting. Cases (a), (b), and (c) correspond to points a, b, and c in Fig. 3. (a) (Top) The unstable synchronous solution and the fast nullcline $h(V)$ of the self-coupled system (4). (Bottom) The coupling term Ω is not strong enough to stabilize the synchronous solution, especially the subthreshold part of the spikes where the coupling is absent. (b) Increasing the inhibition shifts the part of the nullcline $h(V)$ above the threshold closer to the threshold $V = \Theta_s$. However, it makes the amplitude of spikes smaller and leaves the spikes in the region above the threshold where the coupling effectively synchronizes the spikes. Notice the transition from square bursting to plateau bursting. (c) Excessively strong inhibition dominating over excitation has a desynchronizing effect. It still forms plateau bursting in the self-coupled system, governing synchronous bursting, but it creates a vertical part of the nullcline $h(v)$ at $V = \Theta_s$. The bursting trajectory has to follow this part of the nullcline for a while when the cells experience a strong desynchronizing impact (notice the negative peak of Ω at $V = \Theta_s$) and get desynchronized.

term $(g_{\rm exc} + g_{\rm inh})\Gamma(V)$ matters as $\Gamma(V)$ becomes close to 1. The second term is only essential for the values of V, close to the threshold Θ_s as the derivative $\Gamma_V(V)$ is close to the delta function at $V = \Theta_s$. There is practically no coupling between the cells when V is below the synaptic threshold Θ_s. The previous analysis of synchronization in excitatory networks of square-wave bursting cells by means of Lyapunov functions [Belykh *et al.*, 2005; Belykh & Hasler, 2011] suggests that the stabilization of spikes via the coupling $\Omega(V)$ amounts to stabilizing the entire synchronous trajectory, including its subthreshold part.

Notice that the lower part of the spikes lies below the synaptic threshold Θ_s [to the left from Θ_s in Fig. 4(a)(top)] where the synchronizing impact of $\Omega(V)$ is insignificant. Therefore, there is no synchronization for these values of $g_{\rm exc}$ and $g_{\rm inh}$. Figure 4(b) corresponds to synchronized bursting, induced by stronger inhibition [point b in Fig. 3(a)]. In fact, increasing the inhibition has a two-fold effect. It lowers the peak of Ω at $V = \Theta_s$ [Fig. 4(b)], making the contribution of the coupling smaller. However, at the same time it is capable of changing the type of bursting such that the spikes of plateau bursting almost entirely lie in the region above the threshold

where the coupling term Ω stabilizes the (most unstable) spiking part of the trajectory. Hence, the inhibition-induced transition to plateau bursting makes synchronization stable. When the inhibition becomes stronger than the excitation, synchronization loses its stability [see, for example, point c in Fig. 3(a)]. Note that the coupling Ω no longer favors the stability of synchronization at $V = \Theta_s$ as it has a negative peak [Fig. 4(c)]. Moreover, the excessive inhibition pushes the right branch of the nullcline $h(V)$ to the left so that the synchronous trajectory experiences this negative, desynchronizing impact for a long time while crawling along the nullcline up to the right upper knee [see the nonsmooth part of the nullcline in Fig. 4(c)]. This results in desynchronization and the onset of asynchronous bursting in the network.

5. The Role of the Reversal Potential

In this section, we show that similar transitions from square-wave to plateau bursting and windows of induced synchronization also can be observed in the network (1) where the excitatory and inhibitory connections $I^i_{\rm syn} = g_{\rm exc}(E_{\rm exc} - V_i)\Gamma(V_j) + g_{\rm inh}(E_{\rm inh} - V_i)\Gamma(V_j), i, j = 1, 2$ are replaced with two synaptic connections $I^i_{\rm syn} = g_{\rm syn}(E_{\rm syn} - V_i)\Gamma(V_j)$, $i, j = 1, 2$. Depending on the value of the reversal potential $E_{\rm syn}$, these synaptic connections can be excitatory or inhibitory or be of a mixed type when $E_{\rm syn}$ lies somewhere in between the two extremes 10 mV and -75 mV. To some extent, decreasing $E_{\rm syn}$ from 10 mV amounts to increasing the inhibitory connections in the original network (1). Figure 5 shows the dependence of the synchronization threshold coupling $g_{\rm syn}$ on the reversal potential $E_{\rm syn}$. There is an optimal range of $E_{\rm syn}$ close to the synaptic threshold $\Theta_{\rm syn} = -40$ mV and corresponding to significantly improved synchronizability of the network. The vertical boundary of this synchronization region around $\Theta_{\rm syn} = -40$ mV corresponds to the 45° line in Fig. 3(a). In fact, the coupling becomes purely inhibitory for the values $V_i > E_{\rm syn} = \Theta_{\rm syn}$ as the factor $(E_{\rm syn} - V_i) < 0$, and therefore the spikes cannot be robustly synchronized.

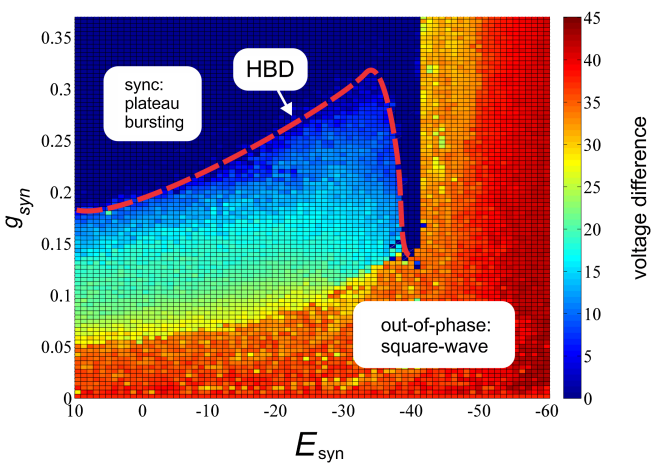

Fig. 5. The stability diagram for synchronization in the network (1) with synaptic connections $I^i_{\rm syn} = g_{\rm syn}(E_{\rm syn} - V_i)\Gamma(V_j)$, $i, j = 1, 2$. The color bar indicates the maximum voltage difference $V_1 - V_2$, calculated over the last two bursts in the established rhythm. Similar to Fig. 3(a), the red dashed curve displays the transition from square-wave to plateau bursting via the disappearance of the homoclinic bifurcation in the fast subsystem. This transition boundary coincides remarkably well with the onset of synchronized bursting. Notice the drop in the coupling strength $g_{\rm syn}$, necessary for inducing synchronization in a window around $E_{\rm syn} = -40$ mV. This window corresponds to the window of induced synchronization in Fig. 3(a).

6. Conclusions

Different types of bursting have significantly different synchronization properties. While square-wave bursters are known for their high resistance to spike synchronization, elliptic and plateau-like bursters are much easier to synchronize and require a weaker coupling strength. Typically, fast nondelayed excitation promotes synchronization of bursters while fast nondelayed inhibition desynchronizes them. Although, counterexamples of synchronizing fast nondelayed inhibition in the weak coupling case have been reported [Jalil *et al.*, 2012]. In this paper, we have shown that the onset of spike synchronization in a network of bursting cells is accompanied by transitions from square-wave to plateau bursting. These transitions can be effectively enhanced by the addition of inhibition to a bursting network with excitatory connections. As a result, the inhibition, that desynchronizes the cells in the absence of excitation, plays a synergetic role and helps the excitation to make synchronization stable. In our study, we have chosen the pancreatic β-cell Sherman model, which exhibits various types of bursting and is capable of switching between them as a building block for the two-cell network. Our preliminary study shows that the reported synergetic effect of combined excitation and inhibition is also present in larger networks of bursting Sherman

models with network topologies admitting complete synchronization. The role of network topology on synchronization of other bursting cell models such as the Hindmarsh–Rose models has been previously studied for excitatory networks [Belykh *et al.*, 2005; Belykh & Hasler, 2011] and for excitatory–inhibitory networks [Belykh *et al.*, 2014], indicating that the number of incoming excitatory and inhibitory connections is often the crucial quantity. A detailed stability analysis of complete synchronization and other phase-locked rhythms in large excitatory–inhibitory networks of Sherman models remains a subject of future work.

Acknowledgments

This work was supported by the National Science Foundation under Grant No. DMS-1009744 and GSU Brains & Behavior program. R. Reimbayev acknowledges support as a GSU Brains & Behavior Fellow.

References

Belykh, V. N., Belykh, I. V., Colding-Jørgensen, M. & Mosekilde, E. [2000] "Homoclinic bifurcations leading to bursting oscillations in cell models," *Eur. Phys. J. E* **3**, 205–219.

Belykh, I., de Lange, E. & Hasler, M. [2005] "Synchronization of bursting neurons: What matters in the network topology," *Phys. Rev. Lett.* **94**, 188101.

Belykh, I. & Shilnikov, A. [2008] "When weak inhibition synchronizes strongly desynchronizing networks of bursting neurons," *Phys. Rev. Lett.* **101**, 078102.

Belykh, I. & Hasler, M. [2011] "Mesoscale and clusters of synchrony in networks of bursting neurons," *Chaos* **21**, 016106.

Belykh, I., Reimbayev, R. & Zhao, K. [2014] "Repulsive inhibition promotes synchrony in excitatory networks: Help from the enemy," (submitted), preprint available at http://www2.gsu.edu/~matixb/research.html

Bertram, R., Butte, M. J., Kiemel, T. & Sherman, A. [1995] "Topological and phenomenologial classication of bursting oscillations," *Bull. Math. Biol.* **57**, 413.

Canavier, C. C., Baxter, D. A., Clark, J. W. & Byrne, J. H. [1999] "Control of multistability in ring circuits of oscillators," *Biol. Cybern.* **80**, 87–102.

Elson, R. C., Selverston, A. I., Abarbanel, H. D. I. & Rabinovich, M. I. [2002] "Inhibitory synchronization of bursting in biological neurons: Dependence on synaptic time constant," *J. Neurophysiol.* **88**, 1166.

Frohlich, F. & Bazhenov, M. [2006] "Coexistence of tonic firing and bursting in cortical neurons," *Phys. Rev. E* **74**, 031922.

Golubitsky, M., Josic, K. & Kaper, T. [2001] "An unfolding theory approach to bursting in fast–slow systems," *Festschrift Dedicated to Floris Takens, Global Analysis of Dynamical Systems*, pp. 277–308.

Guckenheimer, J. & Oliva, R. A. [2002] "Chaos in the Hodgkin–Huxley model," *SIAM J. Appl. Dyn. Syst.* **1**, 105–114.

Hindmarsh, J. L. & Rose, R. M. [1984] "A model of neuronal bursting using three coupled first order differential equations," *Proc. Roy. Soc. London B* **221**, 87.

Izhikevich, E. M. [2000] "Neural excitability, spiking and bursting," *Int. J. Bifurcation and Chaos* **10**, 1171–1266.

Izhikevich, E. M. [2001] "Synchronization of elliptic bursters," *SIAM Rev.* **43**, 315.

Jalil, S., Belykh, I. & Shilnikov, A. [2012] "Spikes matter for phase-locked bursting in inhibitory neurons," *Phys. Rev. E* **85**, 036214.

Kopell, N. & Ermentrout, G. B. [2002] "Mechanisms of phase-locking and frequency control in pairs of coupled neural oscillators," *Handbook of Dynamical Systems*, Vol. 2, ed. Fiedler, B. (Elsevier, Amsterdam), pp. 3–54.

Kopell, N. & Ermentrout, G. B. [2004] "Chemical and electrical synapses perform complementary roles in the synchronization of interneuronal networks," *Proc. Natl. Acad. Sci. USA* **101**, 15482.

Rinzel, J. [1987] "A formal classification of bursting mechanisms in excitable systems," *Mathematical Topics in Population Biology, Morphogenesis, and Neurosciences*, Lecture Notes in Biomathematics, Vol. 71, eds. Teramoto, E. & Yamaguti, M. (Springer-Verlag, Berlin), pp. 267–281.

Rinzel, J. & Ermentrout, B. [1989] "Analysis of neural excitability and oscillations," *Methods in Neuronal Modeling*, eds. Koch, C. & Segev, I. (MIT Press, Cambridge, MA), pp. 251–291.

Rubin, J. & Terman, D. [2002] "Synchronized activity and loss of synchrony among heterogeneous conditional oscillators," *SIAM J. Appl. Dyn. Syst.* **1**, 146.

Sherman, A. [1994] "Anti-phase, asymmetric, and aperiodic oscillations in excitable cells I. Coupled bursters," *Bull. Math. Biol.* **56**, 811–835.

Shilnikov, L. P., Shilnikov, A. L., Turaev, D. V. & Chua, L. O. [1998] *Methods of Qualitative Theory in Nonlinear Dynamics* (*Part I*), World Scientific Series on Nonlinear Science, Ser. A, Vol. 4.

Shilnikov, L. P., Shilnikov, A. L., Turaev, D. V. & Chua, L. O. [2001] *Methods of Qualitative Theory in Nonlinear Dynamics* (*Part II*), World Scientific Series on Nonlinear Science, Ser. A, Vol. 5.

Shilnikov, A. L., Calabrese, R. & Cymbaluyk, G. [2005] "Mechanism of bi-stability: Tonic spiking and bursting in a neuron model," *Phys. Rev. E* **71**, 205.

Shilnikov, A. L. & Cymbaluyk, G. [2005] "Transition between tonic-spiking and bursting in a neuron model via the blue-sky catastrophe," *Phys. Rev. Lett.* **94**, 048101.

Shilnikov, A., Gordon, R. & Belykh, I. [2008] "Polyrhythmic synchronization in bursting network motifs," *Chaos* **18**, 037120.

Shilnikov, A. & Kolomiets, M. [2008] "Methods of the qualitative theory for the Hindmarsh–Rose model: A case study. A tutorial," *Int. J. Bifurcation and Chaos* **10**, 2141–2168.

Stern, J., Osinga, H., LeBeau, A. & Sherman, A. [2008] "Resetting behavior in a model of bursting in secretory pituitary cells: Distinguishing plateaus from pseudo-plateaus," *Bull. Math. Biol.* **70**, 68–88.

Somers, D. & Kopell, N. [1993] "Rapid synchronization through fast threshold modulation," *Biol. Cybern.* **68**, 393.

Terman, D. [1991] "Chaotic spikes arising from a model of bursting in excitable membranes," *SIAM J. Appl. Math.* **51**, 1418–1450.

Terman, D. [1992] "The transition from bursting to continuous spiking in excitable membrane models," *J. Nonlin. Sci.* **2**, 133–182.

Turaev, D. V. & Shilnikov, L. P. [1995] "On a blue sky catastrophe," *Soviet Math. Dokl.* **342**, 596–599.

Tsaneva-Atanasova, K., Osinga, H., Riel, T. & Sherman, A. [2010] "Full system bifurcation analysis of endocrine bursting models," *J. Theor. Biol.* **264**, 1133–1146.

van Vreeswijk, C., Abbott, L. F. & Ermentrout, G. B. [1994] "When inhibition not excitation synchronizes neural firing," *J. Comput. Neurosci.* **1**, 313.

Wang, X.-J. & Rinzel, J. [1992] "Alternating and synchronous rhythms in reciprocally inhibitory model neurons," *Neural Comput.* **4**, 84.

Wang, X.-J. [1993] "Genesis of bursting oscillations in the Hindmarsh–Rose model and homoclinicity to a chaotic saddle," *Physica D* **62**, 263–274.

Wojcik, J., Clewley, R. & Shilnikov, A. [2011] "Order parameter for bursting polyrhythms in multifunctional central pattern generators," *Phys. Rev. E* **83**, 056209.

Wojcik, J., Clewley, R., Schwabedal, J. & Shilnikov, A. [2014] "Key bifurcations of bursting polyrhythms in 3-cell central pattern generators," *PLoS ONE* **9**, e92918.